Downloaded from rsta.royalsocietypublishing.org on March 22, 2011

PHILOSOPHICAL TRANSACTIONS OF THE ROYAL SOCIETY A MATHEMATICAL, PHYSICAL & ENGINEERING SCIENCES

High-energy-resolution monochromator for aberration-corrected scanning transmission electron microscopy/electron energy-loss spectroscopy

Ondrej L. Krivanek, Jonathan P. Ursin, Neil J. Bacon, George J. Corbin, Niklas Dellby, Petr Hrncirik, Matthew F. Murfitt, Christopher S. Own and Zoltan S. Szilagyi

Phil. Trans. R. Soc. A 2009 **367**, 3683-3697
doi: 10.1098/rsta.2009.0087

Supplementary data "Audio Supplement"
http://rsta.royalsocietypublishing.org/content/suppl/2009/08/11/367.1903.3683.DC1.html

References **This article cites 33 articles, 3 of which can be accessed free**
http://rsta.royalsocietypublishing.org/content/367/1903/3683.full.html#ref-list-1

Rapid response Respond to this article
http://rsta.royalsocietypublishing.org/letters/submit/roypta;367/1903/3683

Subject collections Articles on similar topics can be found in the following collections

light microscopy (2 articles)
electron microscopy (21 articles)

Email alerting service Receive free email alerts when new articles cite this article - sign up in the box at the top right-hand corner of the article or click **here**

To subscribe to *Phil. Trans. R. Soc. A* go to:
http://rsta.royalsocietypublishing.org/subscriptions

This journal is © 2009 The Royal Society

Downloaded from rsta.royalsocietypublishing.org on March 22, 2011

PHILOSOPHICAL TRANSACTIONS OF THE ROYAL SOCIETY A

Phil. Trans. R. Soc. A (2009) **367**, 3683–3697
doi:10.1098/rsta.2009.0087

High-energy-resolution monochromator for aberration-corrected scanning transmission electron microscopy/electron energy-loss spectroscopy

By Ondrej L. Krivanek*, Jonathan P. Ursin, Neil J. Bacon, George J. Corbin, Niklas Dellby, Petr Hrncirik, Matthew F. Murfitt, Christopher S. Own and Zoltan S. Szilagyi

Nion Company, 1102 8th Street, Kirkland, WA 98033, USA

An all-magnetic monochromator/spectrometer system for sub-30 meV energy-resolution electron energy-loss spectroscopy in the scanning transmission electron microscope is described. It will link the energy being selected by the monochromator to the energy being analysed by the spectrometer, without resorting to decelerating the electron beam. This will allow it to attain spectral energy stability comparable to systems using monochromators and spectrometers that are raised to near the high voltage of the instrument. It will also be able to correct the chromatic aberration of the probe-forming column. It should be able to provide variable energy resolution down to approximately 10 meV and spatial resolution less than 1 Å.

Keywords: monochromator; electron energy-loss spectroscopy; scanning transmission electron microscope; aberration correction; chromatic correction

1. Introduction

At the Electron Energy Loss Spectroscopy and Imaging (EELSI) meeting held at Port Ludlow, WA, USA, in September 1998, two of the present authors gave a paper entitled 'Towards sub-Å electron beams' (published as Krivanek *et al.* 1999). The smallest electron probe diameter attained up to that time was approximately 1.2 Å, and optimism was therefore needed to justify the title. It was clear that reaching significantly below 1 Å was going to be possible only with aberration correction, and practical aberration correctors were only just beginning to show promise.

The decade that followed justified the optimism many times over. A corrector of spherical aberration ($C_s \equiv C_3$) for a VG Microscopes 120 kV cold field emission (CFE) scanning transmission electron microscope (STEM) produced sub-ångström resolution high-angle annular dark field (HAADF) images less than 4 years later (Batson *et al.* 2002). The probe size was improved to 0.78 Å (at 300 kV primary voltage) soon after (Nellist *et al.* 2004) and is now

*Author for correspondence (krivanek.ondrej@gmail.com).

One contribution of 14 to a Discussion Meeting Issue 'New possibilities with aberration-corrected electron microscopy'.

 This journal is © 2009 The Royal Society

Downloaded from rsta.royalsocietypublishing.org on March 22, 2011

around 0.5 Å, also at 300 kV (Sawada *et al.* 2007, 2008; Kisielowski *et al.* 2008). The currents available in atomic sized probes have also grown remarkably, to approximately 1 nA in 1.5 Å diameter probes at 100 kV (Krivanek *et al.* 2008*a*) and by similar amounts at 300 kV (Watanabe *et al.* 2006). The increased probe current has allowed 256 × 256 pixel atomic resolution elemental maps to be obtained by electron energy-loss spectroscopy (EELS) spectrum imaging in approximately 10 min at 100 kV (Muller *et al.* 2008; L. Fitting-Kourkoutis and D. A. Muller 2009, unpublished data), and X-ray elemental maps with sensitivity close to the single atom level to be acquired (Watanabe *et al.* 2006).

Other areas of electron-optical instrumentation have also seen major advances. Transmission electron microscope (TEM) correctors of spherical aberration have been developed and have produced resolution also approaching 0.5 Å when used with a monochromator that reduces the energy width of the primary beam (Tiemeijer *et al.* 2008). Correctors using combined electrostatic–electromagnetic quadrupoles first suggested by Kel'man & Yavor (1961) have allowed chromatic aberration (C_c) to be corrected along with spherical aberration, first in a scanning electron microscope (Zach & Haider 1995) and more recently in a fixed-beam TEM (Haider *et al.* 2008). A combined $C_s + C_c$ corrector based on an inhomogeneous Wien filter has also been proposed (Rose 1990*a*). These developments are especially important for lower operating voltages, at which chromatic aberration often constitutes the most important resolution limit. Further, monochromators able to reduce the energy width of the primary beam to 0.1 eV and less have been developed (see §2), and spectrometers able to record electron energy-loss spectra with the improved resolution made possible by the monochromators have been designed and built (Su *et al.* 2003; Essers *et al.* 2008).

In this paper we describe the design of a monochromator that should be able to improve both the EELS energy resolution and the long-term EELS energy stability. The monochromator will also be able to correct the chromatic aberration of the STEM probe incident on the sample using a novel correction principle: magnetic sextupoles acting on an energy-dispersed beam. To our knowledge, the principle has never been employed in an electron microscope column, even though it is common practice in particle accelerators (Courant & Snyder 1958; Lee 2004).

2. High-energy-resolution electron energy-loss spectroscopy

Electron energy-loss spectroscopy in the STEM is now an established technique (Egerton 1996, 2005) able to detect single atoms in favourable cases (Krivanek *et al.* 1991; Leapman 2003; Varela *et al.* 2004), produce elemental maps with atomic resolution and explore the nature of the atomic bonds in many types of materials. The EELS energy resolution that can be attained at medium primary voltages (100–300 kV) is approximately 0.1–0.5 eV. It is determined mainly by two parameters: the energy width δE of the primary beam, and the energy resolution of the spectrometer, with the energy width of the beam typically being more limiting. Spectral energy resolutions of approximately 0.3 eV can be obtained with room-temperature tungsten CFE sources run at a small to moderate total beam current (e.g. Garvie & Craven 1994; Batson 2005). Further improvements in the energy resolution are possible with low-workfunction sources (Batson 1987; Fransen *et al.* 1999), but to progress reliably to 0.1 eV energy resolution and below, monochromating the primary beam is required.

Downloaded from rsta.royalsocietypublishing.org on March 22, 2011

Energy resolution of around 0.1 eV makes a major difference for EELS fine-structure studies in materials containing elements such as carbon and silicon, which have energy-loss edges not greatly broadened by a short lifetime of the core hole (Egerton 1996). It also allows more detailed explorations of energy losses of the order of a few electron volts, and thus makes possible studies of band gaps and band-gap defects in semiconductors, and of detailed low-loss structures in materials such as metal nanoparticles (Schaffer *et al.* 2009), insulators and organic materials. Reducing the energy width of the primary beam to 0.1–0.2 eV is also useful for improving the spatial resolution of bright-field images (Tiemeijer *et al.* 2008), which are particularly sensitive to resolution loss due to chromatic aberration, and for improving the resolution of all imaging modes at primary energies smaller than 100 keV.

Several different types of monochromators aiming to combine energy resolution of the order of 0.1 eV with small-probe capabilities have been built in the last decade (Terauchi *et al.* 1999; Tiemeijer 1999; Mook & Kruit 2000; Batson *et al.* 2000; Kahl & Rose 2000; Huber *et al.* 2004 (based on the design of Rose 1990*b*); Mukai *et al.* 2006). All these instruments share one important trait: they disperse the beam in energy when it is at a low voltage of the order of 1–5 keV, and then accelerate it to the final voltage. This arrangement allows them to attain dispersions of the order of tens of micrometres per electron volt, which means that micrometre-sized slits can be used to select energy passbands of the order of 0.1 eV. (The very compact design of Mook and co-workers is an exception—it gives a dispersion of $4.2\,\mu\mathrm{m\,eV^{-1}}$ and uses a 'nanoslit' to select the energy passband.) The energy selection is typically done at the reduced beam energy, except in the Tiemeijer design, in which the beam is dispersed in energy at a reduced voltage, accelerated to the final voltage and only then is the energy selection performed. The high-energy beam being less sensitive to charging at the slit, this arrangement results in the practical advantage that maintaining the slit charge-free becomes less critical.

As another point of comparison, some monochromator systems never cancel the dispersion and therefore illuminate the sample with a beam that is dispersed in energy, whereas more recent monochromators tend to be dispersing–undispersing ones (Kahl & Rose 2000; Huber *et al.* 2004; Mukai *et al.* 2006), in which the beam is dispersed according to its energy in the first half of the monochromator, a small range of energies is selected, and then the dispersion is cancelled in the second half of the monochromator. This makes sure that the beam incident on the sample is not spread in energy, thereby reducing the loss of beam brightness to just the loss inherent to cutting out the parts of the beam outside the selected energy window. In practice, the dispersing–undispersing design preserves about a factor of three times higher brightness than simpler designs that do not cancel the energy dispersion in the beam incident on the sample.

Two of the above monochromators are used together with Wien filter spectrometers that are preceded by electron decelerators, and act on electron beams whose energy has been reduced to a few hundred electron volts (Terauchi *et al.* 1999; Batson *et al.* 2000). The same high-voltage power supply is used for the deceleration as for the microscope's accelerator. This means that instabilities in the 100–120 kV high-voltage power supply do not shift the energy-loss spectra produced by the spectrometer, resulting in very good long-term energy stability of the total system. Unfortunately, this approach is more difficult at

Downloaded from rsta.royalsocietypublishing.org on March 22, 2011

primary voltages of 200 kV and above, for which the high-voltage insulation in the spectrometer (which contains a decelerator plus an accelerator) becomes more complicated.

The other designs use magnetic spectrometers and have no means for linking the energy selected by the monochromator to the energy being resolved by the spectrometer. They therefore rely on the individual stabilities of the high-voltage and spectrometer power supplies for attaining good stability of the dispersed spectra. A change of one part per million (1 ppm) in the high-voltage results in the spectrum shifting by 200 meV in a 200 kV instrument, and a 1 ppm change in the current of a magnetic spectrometer shifts the spectrum by 340 meV in the same instrument. It is a tribute to the stability of present-day power supplies that energy-loss spectra with resolution better than 50 meV have been recorded with short acquisition times in such systems (Essers *et al.* 2008), and it is not surprising that the energy resolution worsens to around 0.1 eV and higher at acquisition times of tens to hundreds of seconds.

If the energy resolution could be improved to around 10 meV, several types of new information would become available in the STEM, including information about the vibrational states of atoms on and in the sample (Ibach 1977). This type of ability was demonstrated by an instrument built by Boersch, Geiger and co-workers in the 1960s and 1970s (Boersch *et al.* 1966; Schröder & Geiger 1972; Geiger 1981). Their spectrometer system used Wien filters acting on a decelerated beam for both the monochromator and the spectrometer and a primary beam voltage of 25–30 kV. Later versions of the instrument attained an energy resolution of 3 meV. The angular resolution was of the order of 0.1 mrad, but the smallest probe that could be formed was larger than 0.1 mm in diameter, and there was no energy-selected imaging capability. In other words, the instrument was an excellent spectrometer, but not a microscope. Vibrational spectra arising from various types of atomic bonds present in hydrogenated amorphous silicon were detected and identified (Geiger 1981). Energy *gain* features were observed in LiF (Boersch *et al.* 1966), arising from fast electrons being accelerated by approximately 50 meV by thermal excitations of the sample. In summary, the Boersch–Geiger spectrometer system pioneered an observational window of fundamentally new capabilities for medium-energy electron beam instruments. It has not been followed up experimentally since.

3. A monochromator combining 10 meV level energy resolution with good spatial resolution

An ideal monochromator/spectrometer system would combine the energy resolution and stability of the Boersch–Geiger instrument with a primary voltage of 100–200 kV, so that samples with realistic thicknesses could be examined. It would also be able to form small probes, so that the spatial distribution of various features appearing in the spectra could be mapped, with enough current for the acquisition of noise-free data on reasonable time scales.

We are now developing a system with such characteristics. As shown in the overall schematic of figure 1, the monochromator precedes the aberration corrector and the objective lens of the STEM, as well as the projector lenses and the final spectrometer. The monochromator and the spectrometer are

Downloaded from rsta.royalsocietypublishing.org on March 22, 2011

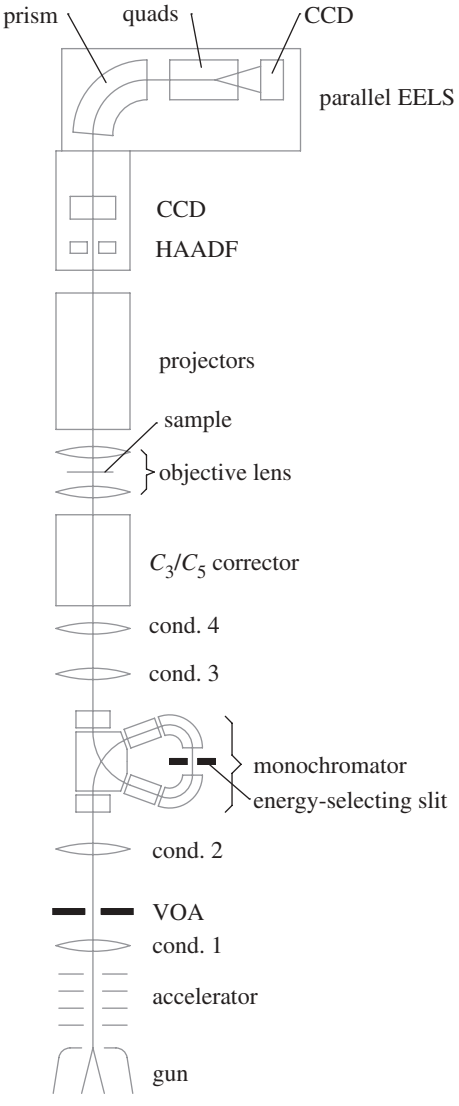

Figure 1. Overall scheme of the monochromated instrument.

both magnetic and act on electrons of the full final energy, i.e. there is no deceleration. The same current is passed through the magnetic prisms of both the monochromator and the spectrometer, with the number of turns in the prism windings in the two parts of the system selected so that the correct bending radii in all the magnetic sectors are produced at the same current value. Small adjustments relative to the linked fields are handled by weak auxiliary windings in the prisms. The results of this arrangement are that the spectrometer tracks whatever energy was selected by the monochromator and that small changes in the prism current or the microscope's high voltage do not produce an energy shift of the final spectrum. Even if the impedances of the windings of the monochromator and the spectrometer are not matched exactly, this affects

Downloaded from rsta.royalsocietypublishing.org on March 22, 2011

only the short-term instabilities, which are much easier to keep under control in all-magnetic systems than long-term drifts. This means that a comparable insensitivity to high-voltage variation should be achieved as with monochromators and spectrometers both raised to near the electron source voltage, but without the inconvenience of having to deal with the high primary voltage in several different places in the instrument.

In order to make sure that the zero loss is accurately centred on the energy-selecting slit, the two halves of the slit are provided with current sensors that allow the system to automatically centre the beam on the slit by adjusting the high voltage as necessary. This arrangement will be able to keep the beam maximum centred on the slit essentially indefinitely. Even if the beam became so mis-centred that no significant current passed through the slit, the arrangement should guarantee that the beam maximum is found quickly and automatically.

The sample is located in the centre of the objective lens of the Nion scanning transmission electron microscope that also includes a C_3/C_5 aberration corrector (Krivanek *et al.* 2008*b*). Probes of less than 1 Å in size can be produced at the sample, with a convergence semiangle of the order of 30–40 mrad. Alternatively, the objective lens can be turned off, which leads to diffraction-limited probes a few tens of nanometres in size, but with the convergence semiangle reduced to as little as 0.01 mrad.

Figure 2 shows a candidate monochromator system, selected from among several different systems that include both alpha- and omega-type filters, whose properties we have analysed computationally. It is a symmetric magnetic alpha filter that produces variable energy dispersion at a slit located in its midplane and then cancels the dispersion in the output beam.

The entrance prism I deflects the beam by 70°, prisms II and III deflect it by 110° each, and then a second passage through prism I deflects it once more by 70°. Figure 3 shows the electron-optical trajectories through the monochromator relative to the curved optical axis of the system. Only the first half of the system is shown; the trajectories through the second half are mirror symmetric about the central (slit) plane. The entrance crossover of the monochromator is an image of the electron source, magnified roughly two times by two condenser lenses, which have a beam-defining aperture (called the 'virtual objective aperture', VOA) located between them. The magnification produces a virtual entrance crossover for the monochromator of approximately 6 nm in diameter, potentially further broadened by the aberrations of the electron gun and the condenser lenses. The total angular divergence at this crossover needed to produce a beam of around 1 nA current at the sample (at 200 kV primary voltage with a CFE source of reduced brightness of $2 \times 10^8\,\mathrm{A\,m^{-2}\,sr^{-1}\,V^{-1}}$ and the energy-selecting slit opened wide) is approximately 1 mrad. The virtual crossover from which the beam appears to emanate is set to 250 mm in front of the first quadrupole, and the beam entering the first quadrupole is therefore approximately 250 μm wide.

The first prism of the monochromator is a uniform-field magnetic sector with a bending radius of 10 cm. It produces an energy dispersion of $0.3\,\mu\mathrm{m\,eV^{-1}}$ at 200 kV primary voltage. Acting together with the two quadrupoles that precede it, the prism demagnifies the virtual source six times, to approximately 1 nm. This means that the energy dispersion in the spectrum produced by the prism that corresponds to one beam diameter is approximately 3 meV. It should therefore be readily possible to select a beam with an energy width of less than 10 meV by a

Downloaded from rsta.royalsocietypublishing.org on March 22, 2011

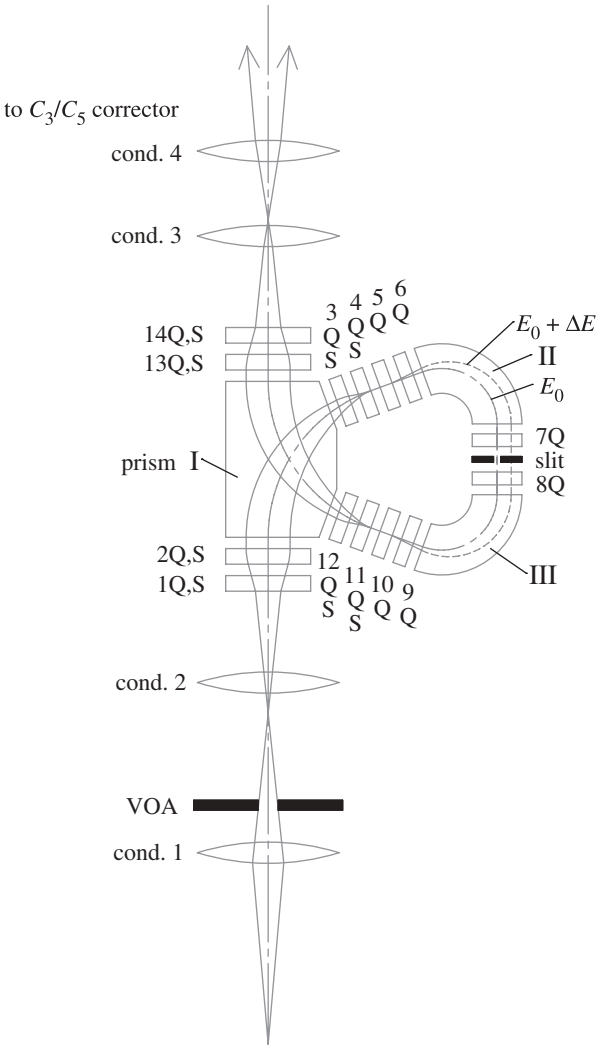

Figure 2. Details of the monochromator design.

suitable slit. However, if the spectrum produced by the prism is not magnified, the slit width would have to be only a few nanometres wide, which is not realistic. A system of four quadrupole lenses situated between prism I and prism II therefore provides a variable magnification of the spectrum from $0\,\mu\mathrm{m\,eV^{-1}}$ (cancelled dispersion) to greater than $200\,\mu\mathrm{m\,eV^{-1}}$. At the high dispersion value, the slit width corresponding to a 10 meV passband is $2\,\mu$m.

After traversing the dispersion-magnifying quadrupoles, the beam enters prism II, which bends it around by 110°, thereby making it antiparallel to the axis of the microscope. Prism II is a gradient-field prism that gives weaker focusing in the x–z plane compared with a uniform-field prism. (See the caption of table 1 for an explanation of the coordinate system and aberration notation used.) At the exit of prism II, quadrupole 7Q fine-tunes the $\mathrm{d}X'/\mathrm{d}E = 0$ first-order constraint that is needed for a mirror-symmetric system that cancels the energy dispersion

Downloaded from rsta.royalsocietypublishing.org on March 22, 2011

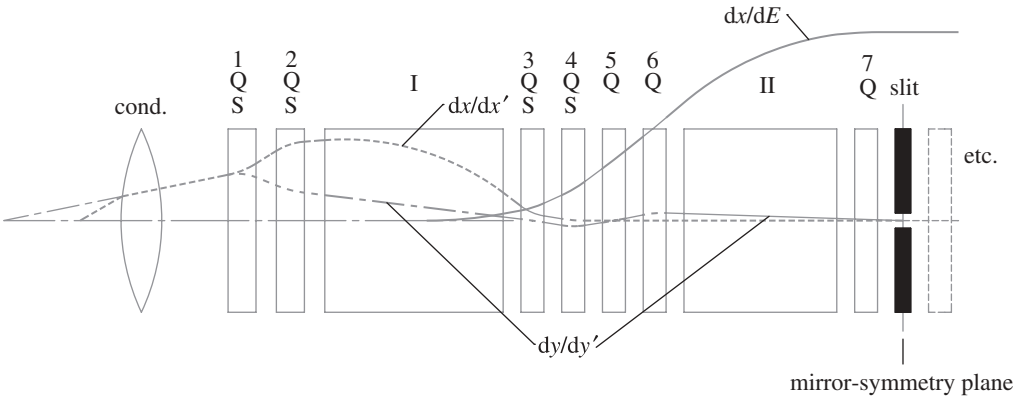

Figure 3. First-order electron-optical trajectories through the monochromator.

Table 1. Requirements for a dispersing–undispersing monochromator. The requirements are specified in the midplane (where the energy-selecting slit is located) as a function of the ray coordinate at the entrance crossover. z is the longitudinal coordinate along the curved central path of the beam; the mirror symmetry plane bisecting the whole monochromator length-wise is $y=0$. x and y are the transverse coordinates of a ray at the entrance crossover of the monochromator. x' and y' are the ray angles with respect to the optic axis at the entrance crossover ($x'=\mathrm{d}x/\mathrm{d}z$). $\mathrm{d}E$ is the energy variation. X, Y, X' and Y' are the coordinates at the energy-selecting slit in the midplane of the monochromator ($z=Z_\mathrm{s}$).

first-order conditions			second-order geometric conditions		second-rank geometric–chromatic conditions	
$\frac{\mathrm{d}X}{\mathrm{d}x'}=0$	$\frac{\mathrm{d}Y}{\mathrm{d}y'}=0$ or $\frac{\mathrm{d}Y'}{\mathrm{d}y'}=0$	$\frac{\mathrm{d}X'}{\mathrm{d}E}=0$	$\frac{\mathrm{d}^2X}{\mathrm{d}x'^2}=0$	$\frac{\mathrm{d}^2X}{\mathrm{d}y'^2}=0$	$\frac{\mathrm{d}^2X}{\mathrm{d}x'\mathrm{d}E}=0$	$\frac{\mathrm{d}^2Y}{\mathrm{d}y'\mathrm{d}E}=0$

in the exit crossover. The beam then traverses the energy-selecting slit located in the midplane of the monochromator. Two other first-order constraints at the slit ($\mathrm{d}X/\mathrm{d}x'=0$ and $\mathrm{d}Y/\mathrm{d}y'=0$) are fine-tuned by the quadrupoles situated between prisms I and II. The first- and second-order optical requirements that need to be satisfied at the midplane are listed in Table 1.

After traversing the energy-selecting slit, the beam enters the mirror-symmetric second half of the monochromator. When it exits from the monochromator, it is free of the first-order energy dispersion.

Choosing $\mathrm{d}Y/\mathrm{d}y'=0$, i.e. making the electrons go through a y crossover at the slit, as in this design, eases the mechanical requirements for slit precision. Choosing $\mathrm{d}Y'/\mathrm{d}y'=0$ (electrons of different starting angles travel parallel to the axis at the slit) provides another mirror-symmetric solution. The second solution reduces stochastic Coulomb effects by avoiding a double crossover in the midplane, but at the cost of increased requirements on the mechanical precision of the slit. Because the whole monochromator is situated after the principal

Downloaded from rsta.royalsocietypublishing.org on March 22, 2011

beam-defining aperture in the column, which reduces the beam current to around 1 nA, and because the electrons travel through the monochromator at their full energy, stochastic Coulomb effects will be unimportant even with the chosen double crossover.

To allow energy selection at the 10 meV level with an entrance beam that is approximately 250 μm wide, the second-order aperture aberrations affecting the spectrum must be corrected. There are four aberrations to correct: the geometric aberrations $\mathrm{d}^2X/\mathrm{d}x'^2$ and $\mathrm{d}^2Y/\mathrm{d}y'^2$, plus the mixed geometric–chromatic aberrations $\mathrm{d}^2X/\mathrm{d}x'\mathrm{d}E$ and $\mathrm{d}^2Y/\mathrm{d}y'\mathrm{d}E$, which are chromatic variations of focus in the x and y directions that manifest themselves as tilts of the spectrum focus plane. In order to make the design more compact and also to make it fine-tunable, we do not use inclined or curved prism faces, which would have provided the first- and second-order focusing of fixed strength. Instead, we use adjustable quadrupoles for setting up the first-order focusing properties of the monochromator, and we correct second-order aberrations that arise in the monochromator's first and last prisms by sextupoles 1S, 2S, 3S and 4S in the first half of the monochromator, plus mirror-symmetric sextupoles in the second half.

The $\mathrm{d}^2X/\mathrm{d}x'\mathrm{d}E$ and $\mathrm{d}^2Y/\mathrm{d}y'\mathrm{d}E$ mixed geometric–chromatic aberrations show up in the rest of the probe-forming column as a mixture of regular chromatic aberration ($C_{\mathrm{c},1,0}$) plus a chromatic change of astigmatism ($C_{\mathrm{c},1,2}$). They are first-order, second-rank aberrations that can be changed by sextupoles acting on an energy-dispersed beam. Energy dispersion set up by the first prism of the monochromator causes ray bundles of different energies to traverse each post-prism sextupole at different locations and thus experience different first-order focusing by the sextupole. This means that the focusing of different energy ray bundles becomes adjustable simply by changing the sextupole strength.

The above correction principle is illustrated in figure 4, which shows the action of a sextupole on a beam dispersed in energy and in angle in the x–z plane. The beam traversing the sextupole is shown as three ray bundles of different energies. When the sextupole is off, the bundles come to focus at different z coordinates, i.e. the plane of the focused spectrum is inclined. When the sextupole is energized appropriately, the bundles come to focus at the same z, giving $\mathrm{d}^2X/\mathrm{d}x'\mathrm{d}E = 0$.

The effectiveness of the $\mathrm{d}^2X/\mathrm{d}x'\mathrm{d}E$ correction varies as $(\mathrm{d}^2x/\mathrm{d}x'^2) * (\mathrm{d}x/\mathrm{d}E)$, and the effectiveness of the $\mathrm{d}^2Y/\mathrm{d}y'\mathrm{d}E$ correction varies as $(\mathrm{d}^2y/\mathrm{d}y'^2) * (\mathrm{d}x/\mathrm{d}E)$. The two aberrations can be corrected simultaneously if a sextupole is placed at a location where $(\mathrm{d}^2x/\mathrm{d}x'^2) * (\mathrm{d}x/\mathrm{d}E)$ is large and $(\mathrm{d}^2y/\mathrm{d}y'^2) * (\mathrm{d}x/\mathrm{d}E)$ is either zero or small, and a second location where the converse holds true. In the present design, the two sextupoles are 3S and 4S. Their action also changes the second-order geometric aberrations $\mathrm{d}^2X/\mathrm{d}x'^2$ and $\mathrm{d}^2Y/\mathrm{d}y'^2$, but the changes are small and easily rectified by sextupoles 1S and 2S.

To correct the chromatic aberrations of the beam leaving the monochromator, mirror-symmetric sextupoles 11S and 12S are needed too. The correction can then also be used to null the C_{c} originating from the rest of the probe-forming column. This allows the monochromator to perform the role of a chromatic aberration corrector of the probe formed at the sample.

Sextupole-based C_{c} correction also produces higher-order effects: the average direction of the energy-dispersed ray bundles is changed, and the focus plane becomes curved (curvature of field). These effects are described by aberration terms $\mathrm{d}^2X/\mathrm{d}E^2$, $\mathrm{d}^2X'/\mathrm{d}E^2$ and $\mathrm{d}^3X/\mathrm{d}x'\mathrm{d}E^2$. The first term is a distortion of

Downloaded from rsta.royalsocietypublishing.org on March 22, 2011

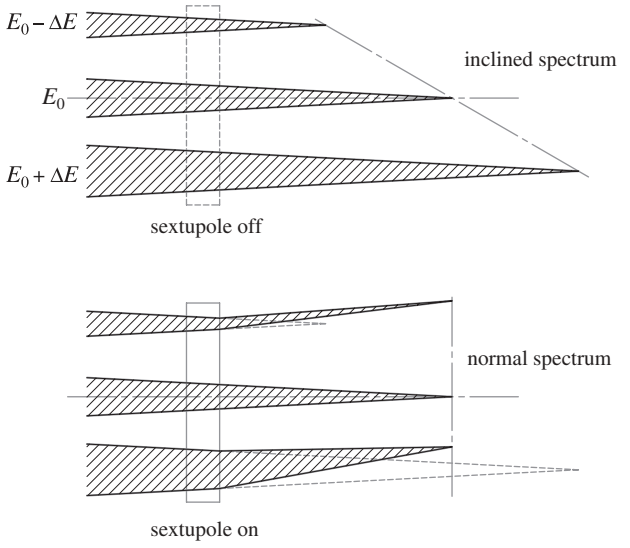

Figure 4. Correction of chromatic aberration by a sextupole acting on an energy-dispersed beam.

the spectrum that does not spoil the mirror symmetry of the monochromator and is therefore of little concern. The second term represents a change in the direction of the ray bundles illuminating the sample. It has no direct effect on the electron probe, and it may be corrected by a sextupole placed either at or near the doubly focused spectrum formed at the energy-selecting slit. The third term is a third-rank aberration that is not expected to be limiting with the narrow energy windows used in a monochromator.

Third-order aberrations produced in the monochromator are small enough not to affect the energy-selecting performance of the monochromator for entrance beam diameters of the order of 250 μm. Third-order to fifth-order geometric aberrations that affect the sample-level probe are corrected by the microscope's C_3/C_5 corrector, which compensates for aberrations arising in the objective lens, the condensers, the gun and now also the monochromator. This leaves mixed chromatic–geometric third-order aberrations as the lowest-order aberrations that are not corrected in the present monochromator. They are not expected to place a major limit on the performance of the total system.

To attain an energy resolution of 10 meV, a high-resolution electron energy-loss spectrometer will be needed to work together with the monochromator. It will have to produce dispersions up to approximately 10 μm meV^{-1} (one CCD channel per 2 meV), i.e. 10 mm eV^{-1}. This is approximately 20 times higher than can be produced with present-day parallel-detection spectrometers such as the Gatan Enfina at 200 kV. Implementing the needed changes in the magnifying optics is fortunately quite straightforward. Furthermore, the isochromaticity of the spectrometer will need to be finely tuned. However, a third-order corrected spectrometer system (i.e. a fourth-order limited system) that can reach 60 mrad acceptance half-angle at the sample while delivering non-isochromaticity of less than 0.4 eV, as can be achieved with a standard Enfina spectrometer and aberration-corrected EELS coupling systems (Krivanek *et al.* 2008*b*), should be

Downloaded from rsta.royalsocietypublishing.org on March 22, 2011

readily able to provide non-isochromaticity of 5 meV for 20 mrad acceptance angle. This will probably be sufficient, given the fact that the highest energy resolutions will be needed only at low energy losses, for which the inelastic scattering angles are typically very small (less than 1 mrad). Note, however, that the usual expression for the characteristic scattering angle applies only to electron–electron scattering and that the angles corresponding to electron–atomic nucleus scattering are much higher. An electron energy-loss spectrometer acting on 100–200 keV primary energy beams that is able to accept high scattering angles at meV-level energy resolution, as needed for vibrational spectroscopy, will require the optics of the spectrometer and its coupling lenses to be highly optimized indeed.

One of the requirements we are placing on the overall system is that it should be easy to retune for more 'regular' EELS of inner-shell losses in the 500 eV–5 keV energy range, for which an energy resolution of the order of 0.3 eV is sufficient. A straight path through the monochromator is therefore provided for this purpose. The instrument will then become an unmonochromated STEM with no loss of brightness due to practical effects such as stray scattering at slit edges, and it will still be able to produce EELS energy resolution of approximately 0.3 eV. For moderate energy resolution improvements, to say 0.1 eV, the monochromation will leave some 30 per cent of the primary electron beam in the monochromated probe. The present design should then allow imaging at essentially the same spatial resolution as in the unmonochromated case, and potentially better spatial resolution at low primary energies, for which correcting the chromatic aberration of the probe-forming column will be especially important.

4. Discussion

Starting with an unmonochromated beam of 1 nA, which is compatible with approximately a 1 Å diameter probe in our instrument (at 200 kV), it should be possible to cut out some 97 per cent of the current, thereby reducing an unmonochromated energy width of 0.3 eV to around 10 meV, and still have a usable probe current of approximately 30 pA for probing vibrational and other ultrafine-structure electron energy-loss spectra. At 10 per cent passband, sufficient for 30 meV energy resolution, the available probe current should be approximately 100 pA. Our system can in theory attain both of these conditions, thereby opening a window on new physics not accessible by present instruments. Among many possible new applications, it should be invaluable for energy-gain spectroscopy using optically induced excitations, recently proposed by García de Abajo & Kociak (2008).

To allow a passband narrower than 10 meV to be selected, as would be useful for in-depth vibrational spectroscopy, the entrance crossover of the monochromator would have to be demagnified more strongly. This is certainly possible with the condenser lenses in the present design. However, to conserve the beam current entering the monochromator, the entrance beam angle would then have to be increased correspondingly. This would make higher-order axial aberrations in the monochromator much more important—e.g. the influence of third-order aberrations would grow 16 times if the entrance beam diameter were doubled.

Downloaded from rsta.royalsocietypublishing.org on March 22, 2011

For pushing below 10 meV energy passbands, it may therefore be necessary to choose either a monochromator design with larger energy dispersion, which will allow larger entrance crossovers to be used, or a design that corrects third- and higher-order monochromator aberrations in addition to second-order ones.

The current in a given-size probe of given angular and energy widths is directly proportional to the brightness of the electron source. Viewed in this light, delivering a probe current that is intense enough for obtaining good statistics in electron energy-loss (or energy-gain) spectra in reasonably short acquisition times is therefore largely a question of source brightness. Because the brightness that matters for the monochromated performance is equal to the beam current per unit area per unit solid angle *per unit energy interval*, CFE electron sources with their intrinsically narrow energy spread will have an even more substantial advantage over Schottky sources than in regular imaging and spectroscopy.

The ability of the monochromator to correct C_c of the probe-forming column, achieved by the correction of all important second-rank aberrations in the monochromator, will be a welcome additional feature. It will of course make little difference to the probe shape when the probe energy spread has been reduced to less than 0.1 eV. However, with the energy-selecting slit open to admit energy widths of 0.2 eV and higher, C_c correction should allow the probe size to be decreased to less than the value available with no monochromator in the column. Provided that the energy-selecting slit intercepts the tails of the energy distribution, the energy-stabilization scheme should then still work, thereby improving long-term spectrum stability. Alternatively, the energy-selecting slit could be opened wide or retracted altogether, thereby avoiding potentially detrimental effects due to scattering at the slit edges. The monochromator would then only function as a C_c corrector. The correction should be especially valuable at primary voltages of 100 kV and less, for which the STEM spatial resolution in C_3/C_5-corrected columns such as the Nion UltraSTEM is presently limited by C_c even with the narrow energy distribution of a cold field emission gun (Intaraprasonk *et al.* 2008; Krivanek *et al.* 2008*a*).

It is also worth keeping in mind that, because the spectrometer part of the total system acts on a beam whose phase space has been greatly increased by scattering in the sample, the electron-optical requirements for the spectrometer are much more demanding than the requirements for the monochromator. This means that in a spectroscopy system in which both the monochromator and the spectrometer act on an electron beam of the full energy, the aberration performance (transmissivity) of the monochromator will typically be less important than that of the spectrometer, and that the spectrometer part of the total system is therefore more likely to be the main limit on the performance of the total system.

5. Conclusions

Aberration correction has given scanning transmission electron microscopes an unprecedented ability to deliver large currents into atom-sized probes. This now makes it feasible to design monochromator/spectrometer systems able to produce 1–2 Å probes of 10–30 meV energy spread with a beam current that is high enough for meaningful electron energy-loss spectroscopy. An instrument able to

Downloaded from rsta.royalsocietypublishing.org on March 22, 2011

do this will provide a revolutionary new capability never before attained with atom-sized electron probes. It should open several new and very exciting windows for studying the atomic-scale properties of materials.

The monochromator will be C_c corrected, and it will also be able to correct the chromatic aberration of the whole probe-forming column. The correction will not require combined electrostatic/electromagnetic quadrupoles, but will use magnetic sextupoles instead. It is expected to be especially useful at low primary voltages, for which it should permit STEM resolutions better than what is possible in non-C_c-corrected columns even with a cold field emission gun with a small energy spread.

Several aspects of the overall performance of the system are likely to depend on factors that are difficult to model, such as the absence of charging at the edges of the monochromator's slit, and adequate immunity to mechanical vibrations. Practical factors of this kind can nearly always be resolved, given enough time and effort. Our optimism level that the proposed monochromator/C_c corrector will be just as successful in reaching its aims as C_s correctors were a decade ago is therefore very high.

References

Batson, P. E. 1987 Low workfunction field emission source for high-resolution EELS. In *Proc. 45th EMSA Meeting* (ed. G. W. Bailey), pp. 132–133. San Francisco, CA: San Francisco Press.

Batson, P. E. 2005 Electron energy loss studies in semiconductors. In *Transmission electron energy loss spectrometry in materials science and the EELS atlas* (ed. C. C. Ahn), pp. 353–384, 2nd edn. Weinheim, Germany: Wiley-VCH.

Batson, P. E., Mook, H. W. & Kruit, P. 2000 High brightness monochromator for STEM. In *Proc. 2nd Conf. Int. Union of Microbeam Analysis Societies* (eds D. B. Williams & R. Shimizu). Institute of Physics Conference Series, no. 165, pp. 231–214. Bristol, UK: Institute of Physics.

Batson, P. E., Dellby, N. & Krivanek, O. L. 2002 Sub-ångström resolution using aberration corrected electron optics. *Nature* **418**, 617–620. (doi:10.1038/nature00972)

Boersch, H., Geiger J. & Stickel, W. 1966 Interaction of 25-keV electrons with lattice vibrations in LiF. Experimental evidence for surface modes of lattice vibration. *Phys. Rev. Lett.* **17**, 379–381. (doi:10.1103/PhysRevLett.17.379)

Courant, E. D. & Snyder, H. S. 1958 Theory of the alternating-gradient synchrotron. *Ann. Phys.* **3**, 1–48. (doi:10.1016/0003-4916(58)90012-5)

Egerton, R. F. 1996 *Electron energy-loss spectroscopy in the electron microscope*, 2nd edn. New York, NY: Plenum.

Egerton, R. F. 2005 Experimental techniques and instrumentation. In *Transmission electron energy loss spectrometry in materials science and the EELS atlas* (ed. C. C. Ahn), pp. 21–48, 2nd edn. Weinheim, Germany: Wiley-VCH.

Essers, E., Mittmann, D., Mandler, T. & Benner, G. 2008 The MANDOLINE filter and its performance. In *Proc. EMC 2008, Aachen,* vol. 1 (eds M. Luysberg, K. Tillmann & T. Weirich), pp. 51–52. Berlin, Germany: Springer.

Fransen, M. J., van Rooy, Th. L. & Kruit, P. 1999 Field emission energy distributions from individual multiwalled carbon nanotubes. *Appl. Surf. Sci.* **146**, 312–327. (doi:10.1016/S0169-4332(99)00056-2)

García de Abajo, F. J. & Kociak, M. 2008 Electron energy-gain spectroscopy. *New J. Phys.* **10,** 073035. See http://www.iop.org/EJ/abstract/1367-2630/10/7/073035.

Garvie, L. A. J. & Craven, A. J. 1994 Use of electron-energy loss near-edge fine structure in the study of minerals. *Am. Mineral.* **79**, 411–425.

Geiger, H. 1981 Inelastic electron scattering with energy losses in the meV-region. In *Proc. 39th EMSA Meeting* (ed. G. W. Bailey), pp. 182–185. Baton Rouge, LA: Claitor's.

Downloaded from rsta.royalsocietypublishing.org on March 22, 2011

Haider, M., Müller, H., Uhlemann, S., Hartel, P. & Zach, J. 2008 Developments of aberration correction systems for current and future requirements. In *Proc. EMC 2008, Aachen,* vol. 1 (eds M. Luysberg, K. Tillmann & T. Weirich), pp. 9–10. Berlin, Germany: Springer.

Huber, A., Bärtle, J. & Plies, E. 2004 Initial experiences with an electrostatic Ω-monochromator for electrons. *Nucl. Instrum. Methods Phys. Res.* **A519**, 320–324. (doi:10.1016/j.nima.2003.11.169)

Ibach, H. 1977 *Electron spectroscopy for surface analysis.* Berlin, Germany: Springer.

Intaraprasonk, V., Xin, H. L. & Muller, D. A. 2008 Analytic derivation of optimal imaging conditions for incoherent imaging in aberration-corrected electron microscopes. *Ultramicroscopy* **108**, 1454–1466. (doi:10.1016/j.ultramic.2008.05.013)

Kahl, F. & Rose, H. 2000 Design of a monochromator for electron sources. In *Proc. EUREM-12, Brno*, vol. 3, pp. 1459–1450.

Kel'man, V. M. & Yavor, S. Ya. 1961 Achromatic quadrupole electron lenses. *Zh. Tekh. Fiz.* **31**, 1439–1442. [Transl. *Sov. Phys. Tech. Phys.* **6**, 1052–1054.]

Kisielowski, C. *et al.* 2008 Detection of single atoms and buried defects in three dimensions by aberration-corrected electron microscope with 0.5-Å information limit. *Microsc. Microanal.* **14**, 469–477. (doi:10.1017/S1431927608080902)

Krivanek, O. L., Mory, C., Tence, M. & Colliex, C. 1991 EELS quantification near the single-atom detection level. *Microsc. Microanal. Microstruct.* **2**, 257–267. (doi:10.1051/mmm:0199100202-3025700)

Krivanek, O. L., Dellby, N. & Lupini, A. R. 1999 Towards sub-Å electron beams. *Ultramicroscopy* **78**, 1–11. (doi:10.1016/S0304-3991(99)00013-3)

Krivanek, O. L, Dellby, N., Keyse, R. J., Murfitt, M. F., Own, C. S. & Szilagyi, Z. S. 2008*a* Advances in aberration-corrected STEM and EELS. In *Aberration-corrected electron microscopy* (ed. P. W. Hawkes). Advances in Electron and Imaging Physics, no. 153, pp. 121–160. Amsterdam, The Netherlands: Elsevier.

Krivanek, O. L., Corbin, G. J., Dellby, N., Elston, B. F., Keyse, R. J., Murfitt, M. F., Own, C. S., Szilagyi, Z. S. & Woodruff, J. W. 2008*b* An electron microscope for the aberration-corrected era. *Ultramicroscopy* **108**, 179–195. (doi:10.1016/j.ultramic.2007.07.010)

Leapman, R. D. 2003 Detecting single atoms of calcium and iron in biological structures by electron energy-loss spectrum-imaging. *J. Microsc.* **210**, 5–15. (doi:10.1046/j.1365-2818.2003.01173.x)

Lee, S. Y. 2004 *Accelerator physics*, 2nd edn. Singapore: World Scientific.

Mook, H. W. & Kruit, P. 2000 Construction and characterization of the fringe field monochromator for a field emission gun. *Ultramicroscopy* **81**, 129–139. (doi:10.1016/S0304-3991(99)00193-X)

Mukai, M. *et al.* 2006 Monochromator for a 200 kV analytical microscope. In *Proc. IMC16, Sapporo*, vol. 1, p. 960.

Muller, D. A., Fitting-Kourkoutis, L., Murfitt, M. F., Song, J. H., Hwang, H. Y., Silcox, J., Dellby, N. & Krivanek, O. L. 2008 Atomic-scale chemical imaging of composition and bonding by aberration-corrected microscopy. *Science* **319**, 1073–1076. (doi:10.1126/science.1148820)

Nellist, P. D. *et al.* 2004 Direct sub-angstrom imaging of a crystal lattice. *Science* **305**, 1741–1742. (doi:10.1126/science.1100965)

Rose, H. 1990*a* Inhomogeneous Wien filter as a corrector compensating for the chromatic and spherical aberration of low-voltage electron microscopes. *Optik* **84**, 91–107.

Rose, H. 1990*b* Electrostatic energy filter as monochromator of a highly coherent electron source. *Optik* **85**, 95–98.

Sawada, H. *et al.* 2007 Achieving 63 pm resolution in scanning transmission electron microscope with spherical aberration corrector. *Jpn. J. Appl. Phys.* **46**, L568–L570. (doi:10.1143/JJAP.46.L568)

Sawada, H. *et al.* 2008 Performance of R005 microscope and aberration correction system. In *Proc. EMC 2008, Aachen,* vol. 1 (eds M. Luysberg, K. Tillmann & T. Weirich), pp. 47–48.

Schaffer, B., Riegler, K., Kothleitner, G., Grogger, W. & Hofer, F. 2009 Monochromated, spatially resolved electron energy-loss spectroscopic measurements of gold nanoparticles in the plasmon range. *Micron* **40**, 269–273. (doi:10.1016/j.micron.2008.07.004)

Schröder, B. & Geiger, J. 1972 Electron-spectrometric study of amorphous germanium and silicon in the two-photon region. *Phys. Rev. Lett.* **28**, 301–303. (doi:10.1103/PhysRevLett.28.301)

Downloaded from rsta.royalsocietypublishing.org on March 22, 2011

Su, D. S. *et al.* 2003 High resolution EELS using monochromator and high performance spectrometer: comparison of V_2O_5 ELNES with NEXAFS and band structure calculations. *Micron* **34**, 235–238. (doi:10.1016/S0968-4328(03)00033-7)

Terauchi, M., Tanaka, M., Tsuno, K. & Ishida, M. 1999 Development of a high energy resolution electron energy-loss spectroscopy microscope. *J. Microsc.* **194**, 203–209. (doi:10.1046/j.1365-2818.1999.00450.x)

Tiemeijer, P. C. 1999 Operation modes of a TEM monochromator. *Proc. EMAG '99, Sheffield.* Institute of Physics Conference Series, no. 161, pp. 191–194. Bristol, UK: Institute of Physics.

Tiemeijer, P. C., Bischoff, M., Freitag, B. & Kisielowski, C. 2008 Using a monochromator to improve the resolution in focal-series reconstructed TEM down to 0.5 Å. In *Proc. EMC 2008, Aachen*, vol. 1 (eds M. Luysberg, K. Tillmann & T. Weirich), pp. 53–54.

Varela, M. *et al.* 2004 Spectroscopic imaging of single atoms within a bulk solid. *Phys. Rev. Lett.* **92**, 095502. (doi:10.1103/PhysRevLett.92.095502)

Watanabe, M., Ackland, D. W., Burrows, A., Kiely, C. J., Williams, D. B., Krivanek, O. L., Dellby, N., Murfitt, M. F. & Szilagyi, Z. 2006 Improvements in the X-ray analytical capabilities of a scanning transmission electron microscope by spherical-aberration correction. *Microsc. Microanal.* **12**, 515–526. (doi:10.1017/S1431927606060703)

Zach, J. & Haider, M. 1995 Correction of spherical and chromatic aberration in low voltage SEM. *Optik* **98**, 112–118.